Expanding the polymethine paradigm: evidence for the contribution of a bis-dipolar electronic structure.

Simon Pascal, Alexandre Haefele, Cyrille Monnereau, Azzam Charaf-Eddin, Denis Jacquemin, Boris Le Guennic, Chantal Andraud, Olivier Maury

Expanding the Polymethine Paradigm: Evidence for the Contribution of a Bis-Dipolar Electronic Structure

Simon Pascal,[a] Alexandre Haefele,[a] Cyrille Monnereau,[a] Azzam Charaf-Eddin,[c] Denis Jacquemin,[c,d] Boris Le Guennic,*[b] Chantal Andraud*[a] and Olivier Maury*[a]

[a] *Université de Lyon, Laboratoire de Chimie, Laboratoire de Chimie, UMR 5182 CNRS-ENS Lyon-Université Lyon 1, 46 Allée d'Italie, 69364 Lyon Cedex 07, France*
E-mail: olivier.maury@ens-lyon.fr, chantal.andraud@ens-lyon.fr

[b] *Institut des Sciences Chimiques de Rennes, UMR 6226 CNRS, Université de Rennes 1, 263 Avenue du Général Leclerc 35042 Rennes Cedex, France*
E-mail: boris.leguennic@univ-rennes1.fr

[c] *Laboratoire CEISAM-CNRS 6230, Université de Nantes, 2 Rue de la Houssinière, BP 92208, 44322 Nantes Cedex 3, France*

[d] *Institut Universitaire de France, 105 Bd Michelet, 75005 Paris Cedex 5, France.*

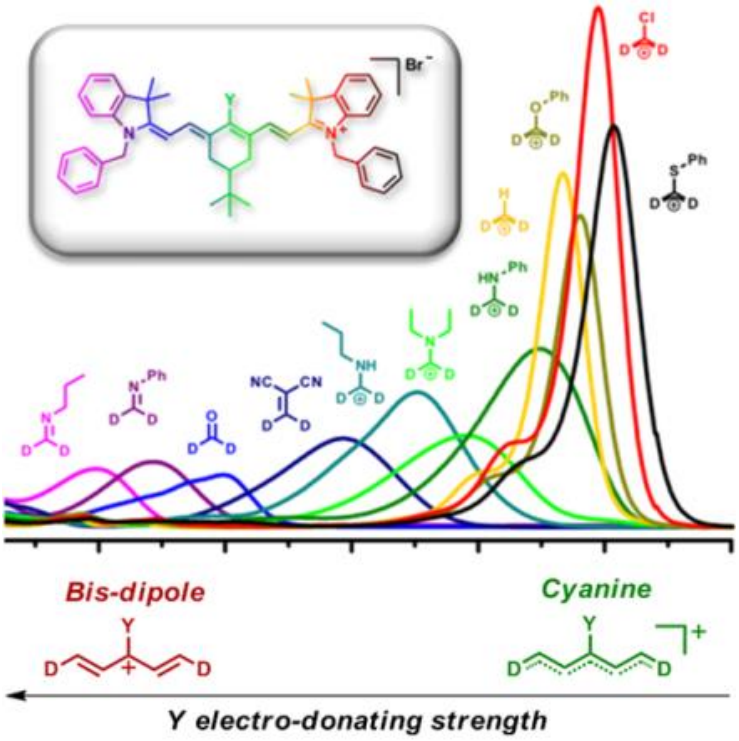

ABSTRACT

Although it has been reported on few instances that the spectroscopic properties of cyanine dyes were strongly dependent on the nature of the chemical substitution of their central carbon atom, there has not been to date any systematic study specifically aimed at rationalizing this behavior. In this article, such a systematic study is carried out on an extended family of 17 polymethine dyes carrying different substituents on their central carbon, some of those being specifically synthesized for this study, some of those similar to previously reported compounds, for the sake of comparison. The evolution of their absorption properties, which spread over the whole visible-near infrared spectral range are seen to be dramatically dependent on the electron-donating character of this central substituent. By correlating this behavior to NMR spectroscopy and (vibronic) TD-DFT calculations, we show that it results from a profound modification of the ground state electronic configuration, namely a progressive localization of the cationic charge on the central carbon as the electron-donating nature of the central substituent is increased.

KEYWORDS

Polymethine dyes, Cyanine limit, Near-infrared dyes, Spectroscopy, TD-DFT

INTRODUCTION

Old polymethine dyes, discovered in the middle of the XIXth century for photography application, continue to hold a real fascination in the scientific community owing to their unique spectroscopic properties.[1-5] In the last decade, these dyes found a renewal of interest for near-infrared (NIR) applications in biological imaging[6, 7] or for the design of advanced photonic materials (laser dyes, nonlinear optics…).[1-5, 8, 9] Generally speaking, polymethine dyes are charged compounds where the positive (resp. negative) charge is delocalized between two electron-donating (resp. withdrawing) groups via an odd number of sp2 carbon atoms.[1, 2, 10] In spite of their wide range of use, the complete rationalization of their very particular photophysical properties remains a matter of debate from both experimental and theoretical points of view.

Recently, by analogy with quadupolar dye,[11] Van Stryland and co-workers proposed to rationalize the spectroscopic properties of polymethine dyes on the basis of three electronic states: a doubly degenerated dipole state where the charge is localized on one extremity and a charge-centered state.[12] The relative energies of the three states determine the nature of the ground state and consequently the spectral properties of the dyes. This approach explained the different behaviors observed in solution that correspond to different ground state electronic configurations, namely:

(i) The cyanine configuration, introduced by Dähne in the early 70's[13, 14] corresponds to a strong mixture of the three aforementioned states (Form I, Figure 1). Consequently the charge is fully delocalized in a symmetric way over the entire conjugated backbone and the bond-length alternation (BLA) is negligible.[15] This cyanine electronic structure is characterized by a sharp, exceptionally intense absorption, located for heptamethines in the NIR spectral range with a vibronic shoulder at higher energy.

(ii) The dipolar configuration (Form II, Figure 1) where the charge is predominantly localized at one extremity resulting in both ground state symmetry breaking and a positive BLA. This dipolar electronic structure is characterized by a broad, structureless charge transfer type transition that is blue shifted compared to the cyanine one. It is possible to change the contribution of each electronic configuration, in other words to "cross the cyanine limit" (forms I→II), by increasing the chain length of the conjugated

skeleton as in the pioneering works of Brooker[16] and Tolbert,[17] by increasing the solvent polarity[18, 19] or by ion-pairing effect.[20, 21] On the other hand, Würthner and co-workers demonstrated that it is possible to cross the cyanine limit in the opposite direction (forms II→I) starting from a dissymmetric dipolar polymethine and increasing the solvent polarity.[22-24]

In the present contribution, we experimentally illustrate the existence of a third electronic configuration of polymethine dyes, corresponding to a predominant charge-centered state called bis-dipole[25] (form III, Figure 1). This electronic configuration is reminiscent of that of V-shaped chromophores;[26, 27] it remains C_{2v}-symmetric but exhibits positive BLA and is associated to a broad charge transfer transition. Using a combined theory-experiment approach on cationic heptamethine dyes, we show that it is possible to tune the ground state configuration from cyanine to bis-dipole (forms I⇆III) by rational variation of the nature of the central substituent Y. To that end, a series of cationic heptamethine **1-10** (Figure 1) has been prepared with a wide range of Y substituents namely, Cl, Br, SPh, OPh, OAc, H and various secondary, tertiary and aromatic amino, alongside with neutral heptamethine **11-14** featuring keto, malonitrile and imino functionalities. Their absorption spectra are spread over the whole visible-NIR range illustrating the dramatic influence of the Y substituent on the ground state electronic configuration. These data were compared to three independent parameters representative for the charge (de)localization: (i) the ^{13}C NMR chemical shift, (ii) the density functional theory (DFT) calculated BLA and (iii) the calculated charge at the central position (Cα) of the bridge.

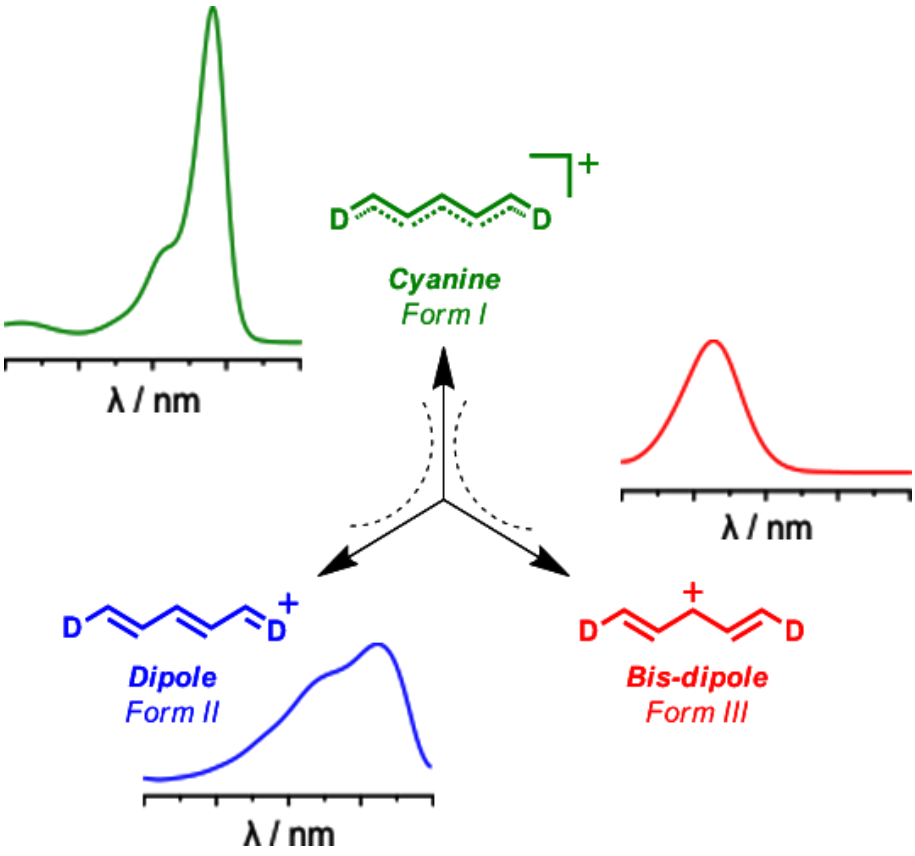

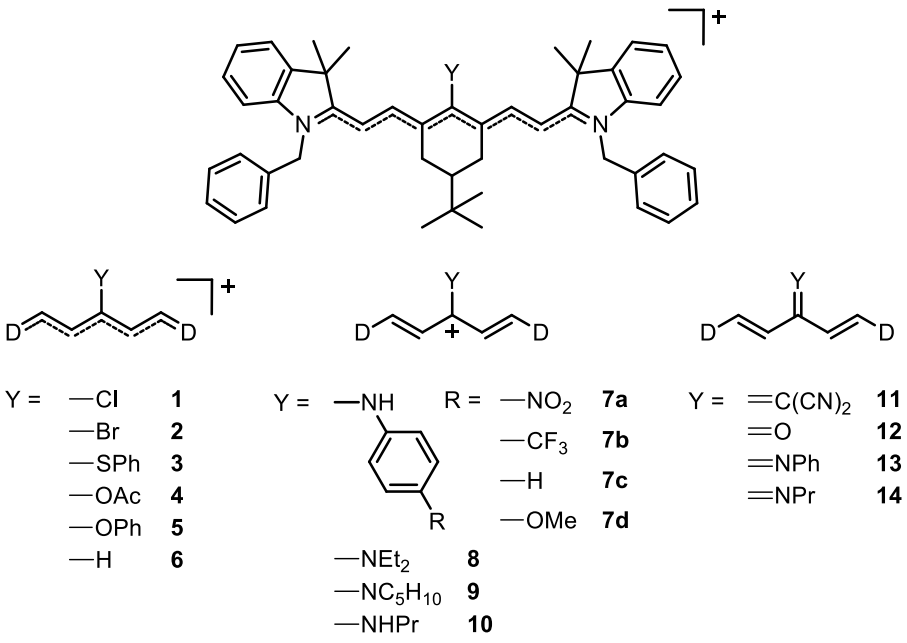

Figure 1. (top) Three electronic configurations of polymethine dyes and their respective absorption profile and (bottom) structure of the heptamethine dyes involved in this study.

RESULTS

Synthesis. The substitution of heptamethines at the central position has been widely studied.[28] The present homogeneous series of **17** polymethines reproduced already existing substitutions using synthetic protocols inspired by the literature, but also described original substitutions like for compounds **2**, **7a,b,d, 11**, **13** and **14**. Experimental details and complete characterization of all chromophores are given in the experimental section and in supporting information. The synthesis of all derivatives used chloro- (resp. bromo-) heptamethine **1**, (resp. **2**) as starting material (Figure 2), that were prepared by a Knoevenagel reaction between a chloro-, (resp. bromo) bis-aldehyde and an indolenium salt in basic, anhydrous conditions.[29] Heptamethines **3** and **5** were obtained under mild conditions as characteristic green powders with metallic shine by reacting **1** with thiophenol or phenol in the presence of caesium carbonate.[30-32] Alkylamino-substituted heptamethines **8**, **9** and **10** were synthesized as glossy blue solids by heating **1** in the presence of the corresponding amine (Et_2NH, piperidine, $nPrNH_2$) in DMF according to the procedure reported by Peng et al.[33] Aniline substituted derivatives **7a-d** were synthesized using a similar procedure.[34] It is worth noting that **7a,b** incorporating electron-deficient substituents required the use of micro-waves heating in a sealed tube to achieve the nucleophilic substitution in moderate yields. Heptamethine **6** was obtained by an original reductive debromination of **2** in the presence of sodium ethanethiolate in ethanethiol. The keto-derivative **12** was synthesized according to the procedure described by Strekowski and co-workers[35] and was further used as precursor for the preparation of the ester derivative **4** by addition of acyl chloride at 0°C.[6] Compound **11**, bearing dicyanovinyl fragment was readily obtained by reaction of **1** with malononitrile in DMF.[36] Finally, in situ deprotonation of secondary amine-based heptamethines **7c** and **10** by treatment with 1M aqueous NaOH or K_2CO_3 solution led to the formation of neutral imine-substituted dyes **13** and **14**, respectively. All chromophores were characterized by HRMS, ^1H and ^{13}C NMR spectroscopy. ^1H NMR analyses unambiguously established that all compounds, regardless of the central substituent, are symmetric and present a all-trans configuration ($^3J_{trans}$ ~ 12-14 Hz).

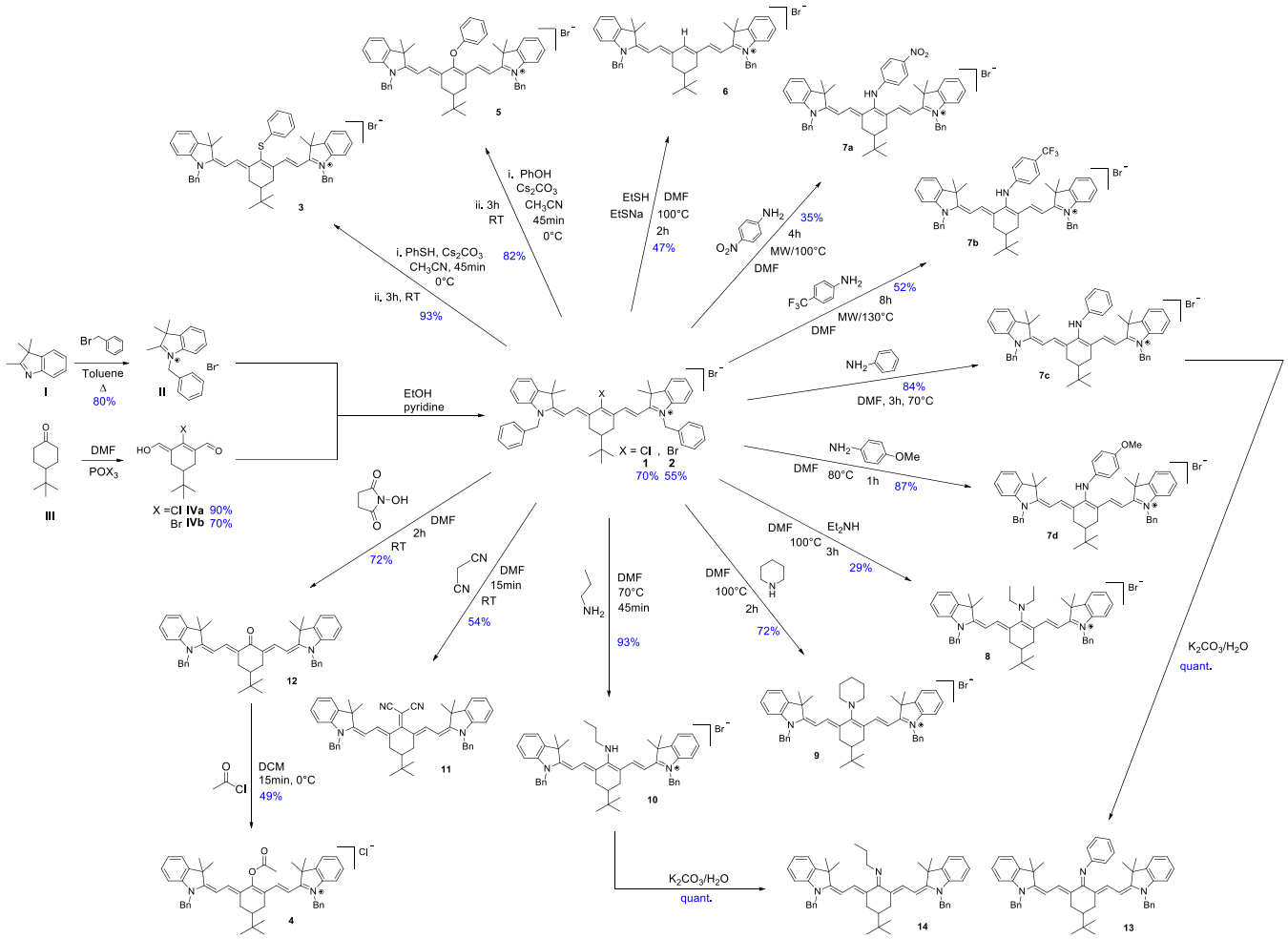

Figure 2. Synthetic scheme for compounds **1-14**.

Absorption properties. All compounds were studied by absorption spectroscopy in diluted dichloromethane or methanol solutions (Figure 3 and Tables 1). Interestingly, in spite of strong structural similarities, chromophores **1-14** exhibit very different absorption spectra, whose maxima are spread over the 400-800 nm range. This feature highlights the dramatic influence of the central substitution on the electronic structure of these molecules. At first glance, two main behaviors can be distinguished: (i) heptamethines **1-6** with intense, sharp and non solvatochromic (Figure S1) *cyanine*-type electronic transitions, all localized in a narrow near-infrared region (750-820 nm); (ii) heptamethines **7-14** with less intense, broad transitions covering the whole visible range (400-750 nm), indicating a loss of *cyanine* character. This transition exhibit a positive solvatochromism as illustrated on **11** (Figure S1). In particular,

neutral heptamethines **11-14** with a central double bond undergo the strongest hypso- and hypochromic effects within the series. It can be noticed that the absorption of aniline-substituted compound **7c** in dichloromethane (Figure 3, top) is located close to the frontier between the two above-mentioned tendencies. Fine modulation of the electronic density of aniline by introduction at the *para* position of electron-donating or -withdrawing moieties allows exploring more specifically this region-of-interest. For solubility reason (Figure S2), the absorption spectra of heptamethines **7a-d** were recorded in diluted methanol solutions and compared to those of **1** and **10**, which are the hallmarks of the *cyanine* and non-*cyanine* behaviors, respectively. Whereas an electron-donating methoxy substituent on the aniline moiety (**7d**) induces a blue-shift of the absorption maximum, the opposite effect is observed for electron-withdrawing trifluoromethyl or nitro substituted derivatives **7a-b**. In addition, along this series, decreasing the electron density on the nitrogen atom induces a progressive hyperchromic effect accompanied by a sharpening of the transition as illustrated by the strong decrease of full width at half maximum, $\omega_{1/2}$ from 2521 to 925 cm^{-1} for **7d** and **7a**, respectively (Table S2), bridging the gap between **10** and **1** ($\omega_{1/2}$ = 2688 and 768 cm^{-1}, respectively). In striking contrast with **7b-d**, **7a**, featuring the strongest electron-withdrawing nitro group, presents an absorption profile with an additional shoulder at higher energy, which further corroborates the *cyanine* character of the associated electronic transition.

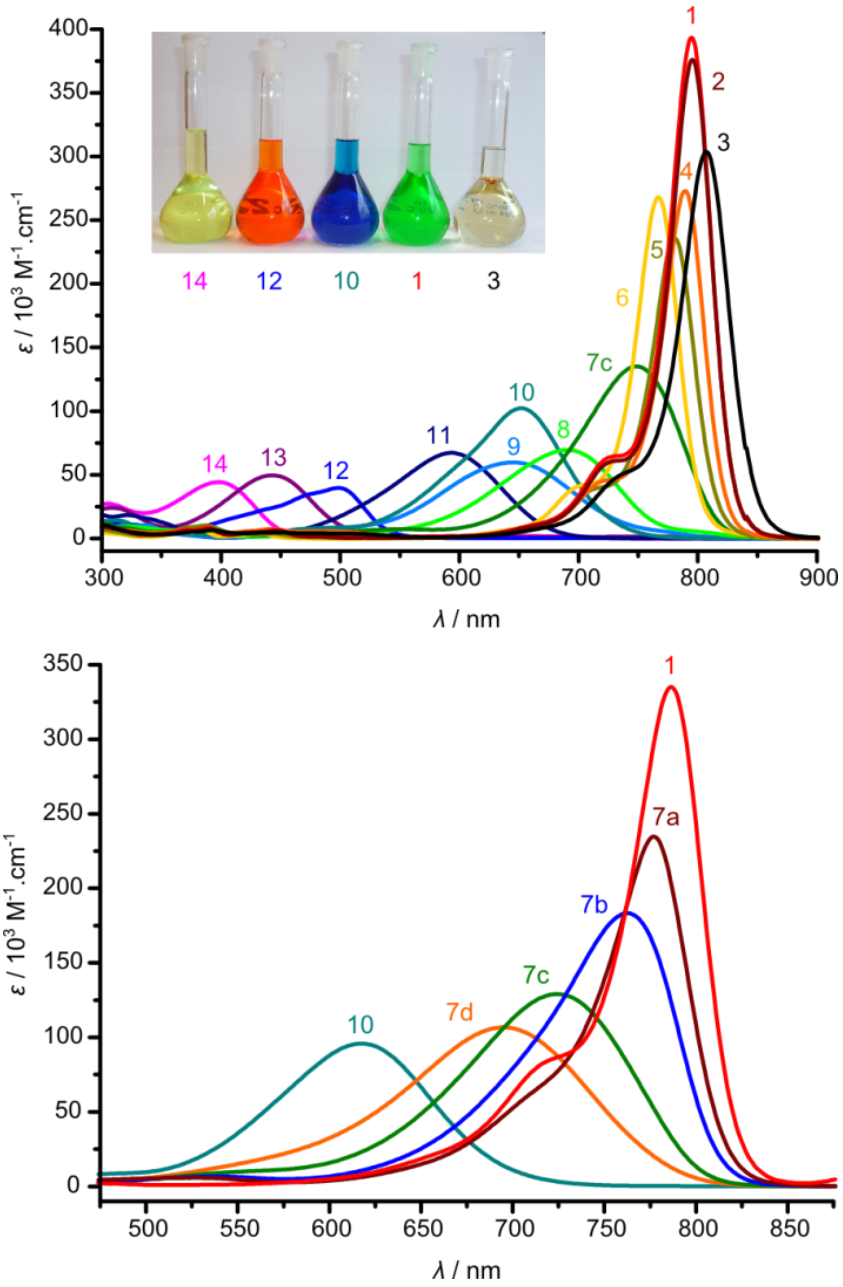

Figure 3. Absorption spectra of heptamethine dyes **1-6**, **7c**, **8-14** in dichloromethane at room temperature (top). Absorption spectra of aniline-derivatives **7a-d** featuring -NO_2 (a), -CF_3 (b), -H (c) and -OMe (d) substituents in methanol at room temperature. Spectra of **1** and **10** in methanol were added for comparison (bottom).

Table 1. Absorption maximum, ^{13}C NMR chemical shift, theoretical bond length alternation and central charge determined for heptamethines **1-14**.[a]

	λ_{abs}, nm	ε, 10^3 $M^{-1}.cm^{-1}$	^{13}C δ, ppm	BLA, Å (M06-2X)	Charge, e^- (M06-2X)
1	795	393	172.4	0.003	4.37
	786[b]	335[b]	174.4[b]		
2	795	376	172.6	0.001	4.35
3	807	304	172.4	0.004	3.86
4	789	273	172.0	0.002	4.36
5	780	236	172.1	0.002	4.29
6	767	268	171.5	0.002	3.77
	754[b]	234[b]	172.9[b]		
7a	777[b]	235[b]	172.9[b]	0.004	4.20
7b	763[b]	183[b]	173.5[b]	0.011	4.10
7c	748	135	172.9[b]	0.016	3.92
	724[b]	129[b]			
7d	695[b]	107[b]	171.8[b]	0.020	3.82
8	690	70	169.1	0.021	3.63
	685[b]	79[b]	170.7[b]		
9	646	60	167.2	0.024	3.46
10	652	102	166.0	0.027	3.36
	627[b]	96[b]	168.8[b]		
11	593	67	163.8	0.037	2.80
12	499	40	162.0	0.065	2.33
13	442[c]	50[c]	158.2[c]	0.072	1.93
14	398[c]	44[c]	156.5[c]	0.083	1.23

[a] Unless stated otherwise, all data were measured/calculated using CH_2Cl_2 as solvent ($CDCl_3$ for NMR data). [b] Measured in MeOH (CD_3OD for NMR data). [c] Measured *in situ* by treatment with 1M aqueous K_2CO_3 or NaOH solution.

To rationalize the influence of the central substitution, we propose the following model: increasing the electron-donating ability of the central substituent Y progressively localizes the cationic charge on the central carbon atom of the polymethine chain. As a result, the delocalization of the charge on the π-conjugated skeleton is reduced and the cyanine character is lost. Instead, a bis-dipole electronic state is reached, which can be described as a central cationic acceptor bearing two electron-donating extremities (Figure 4). Within this model, polymethines **1-6** show a clear cyanine character, while dyes **7c-14** fall into the bis-dipole category.

At the frontier, intermediate behaviors are observed for **7a** and to a less extent **7b**, which correspond to the so-called *cyanine limit*. At the other extremity, neutral polymethines **11-14** can be depicted under their limit form where an anionic substituent faces a central highly localized carbocation (Figure 4). This model is in line with the explanation proposed by Marder and co-workers in the particular case of a dimethylamine-substituted polymethines.[37]

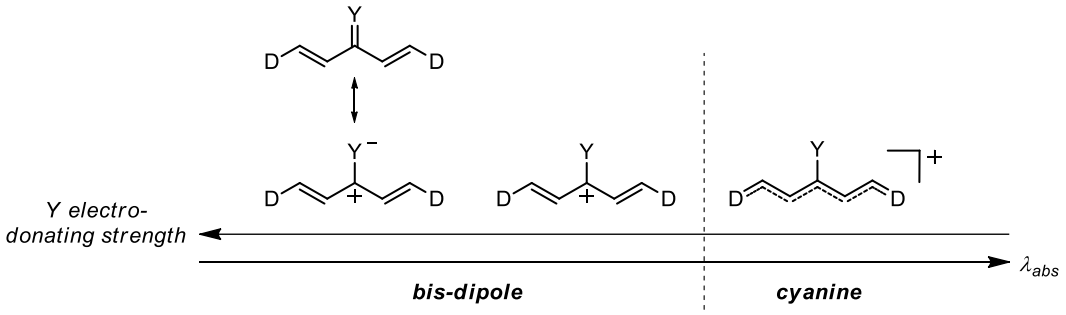

Figure 4. Electronic structure model showing the stabilization of the cationic charge at the central position as Y electron-donating strength increases.

Theoretical calculations. In a first approach, time-dependent density functional theory (TD-DFT) calculations were performed on the ground state optimized geometries of compounds **1** and **12** representatives for the *cyanine* and *bis-dipole* electronic configuration, respectively (see experimental

section for computational details). The purpose was to identify the nature of the transitions involved in the cyanine and bis-dipole behaviors, and verify that those were in agreement with our proposed model.

In the past, the intriguing optical properties of cyanine dyes have excited theoretical chemists who applied more or less sophisticated methodologies to deal with the computation of BLA, electronic excitation energies or second- and third-order polarisability.[38-43] In particular, numerous works were devoted to the question of the non-pertinence of TD-DFT for a correct description of electronic excitations energies in cyanine dyes.[44, 45] As expected, vertical TD-DFT calculations do not properly reproduce the experimental λ_{max} of the *cyanine* class,[46] whereas there are in excellent agreement in the case of **12** featuring a strong *bis-dipole* character (Table S3). In Figure 5, the density difference plots for these two compounds illustrates, on the one hand, the cyanine character of **1** with alternating regions of gain/loss of electron density presenting similar spatial extend. On the other hand, the *bis-dipole* nature of **12** is confirmed with a red electron accepting zones (resp. blue electron donating regions) mainly localized at the center (resp. extremities) of the dye, though the usual red/blue alternating pattern, typical of transitions implying π electrons, pertains. In order to gain further insights on the origin of the evolution of the band shapes when crossing the *cyanine limit*, we determined vibronic spectra for **1** and **12** (Figure 5). First, we underline that the qualitative match with experimental absorption profiles of Figure 3 is remarkable, with **12** presenting a less intense and broader absorption profile located at higher energies. In comparison, the absolute transition energies of **1** are not very accurate, a known problem with vertical TD-DFT (see above). Secondly, these simulations allowed identifying the vibrational modes responsible for the broadened shape of **12** and the hallmark shape of **1**. For the latter, the band asymmetry is explained by a series of low-frequency deformations, the 178th mode (1730 cm^{-1}) that corresponds to an asymmetric change of the character of the bonds in the conjugated pathway being relatively weakly coupled. In **12**, the 135th (1383 cm^{-1}) and 172th (1568 cm^{-1}) vibrational modes, mainly responsible for the emergence of the second peak, imply symmetric change of the single/double character of the bonds. Obviously such modes are more important when the BLA significantly departs from zero, which is consistent with their key role in **12** and their absence in **1**.

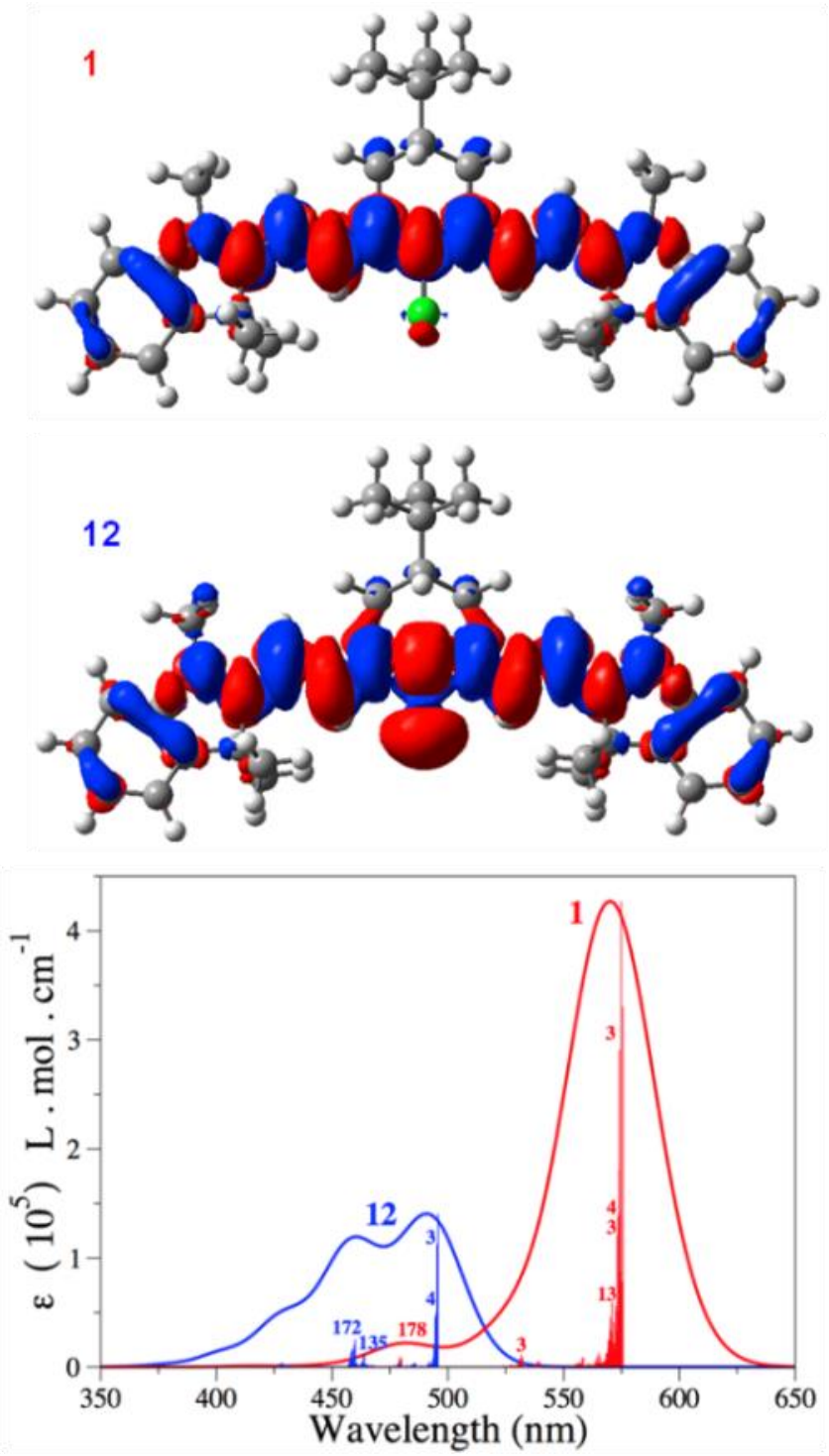

Figure 5. Density difference plots for the first excited state of **1** and **12** (top). The red (blue) zones indicate increase (decrease) of density upon electronic transition. Simulated vibrationally resolved spectra of **1** and **12** (bottom). For each system, the excited-state vibrational modes that strongly contribute to the band shape are displayed.

Discussion

To further validate our model, we investigated three additional parameters related to the charge (de)localization: (i) the experimental ^{13}C NMR chemical shift that is correlated to the electron density on an atom, (ii) the BLA, a well-known structural measure of the electronic delocalization, obtained on DFT optimized structures, and (iii) the calculated charge at the central position (C_α) of the bridge.

We screened the charge density by measuring the ^{13}C chemical shift (δ) of the C_ω carbon at the extremity of the heptamethine bridge (Table 1, Figures 6).[47] According to our model, the progressive localization of the positive charge at the central C_α carbon towards a *bis-dipole* electronic structure should result in a higher electron density on the indolenine donor extremities of the molecule and consequently a larger shielding of the C_ω NMR signal. Experimentally, a 172 +/- 0.5 ppm chemical shift is recorded for all dyes **1-6** exhibiting a *cyanine*-like absorption, signature of a perfect delocalization of the charge. As predicted, when the electron-donating strength of the central substituent increases, the signal is progressively shielded from 171 ppm for dye **7c** to *ca.*157 ppm for imine **14**.

This experimental observation is in agreement with the evolution of the APT charge (see Computational Details section) borne by the central C_α carbon atom calculated at the PCM(DCM)-M06-2X/6-311G(2d,p) level (Table 1). Similar results are obtained with both PBE0 and ωB97X-D functionals or with MeOH as solvent (Tables S4-6 and Figures S3-4). Once again, *cyanine* type compounds **1-6** present similar central charges with an average value of 4.17 *e*. The aniline derivative **7c**, with a charge of 3.92 *e*, exhibits an intermediate value between the *cyanine* and *bis-dipole* forms, while the *bis-dipole* dyes **8**-**14** cover a wide range of values, with decreasing charge from 3.36 *e* for the amine derivative **10**, to 1.23 *e* for the corresponding imine **14**. These data are consistent with our model since they indicate a progressive localization of the cationic charge at the center, thereby decreasing the electron density at C_α position. Finally, the BLA calculated on the optimized geometries allows discriminating between *cyanine* (BLA ~ 0) and *bis-dipole* (BLA > 0) electronic structures (Table 1). As expected, **1-6** show a BLA very close to zero,

whereas it progressively increases from **7** to **14** as the double bonds localize at the C_β-C_γ and C_δ-C_ω positions.

The validity of our model is further confirmed by the remarkable linear correlations that exist between the selected parameters representative for the degree of charge (de)localization ($\delta(^{13}C)$, BLA, charge) and the lowest transition energy (Figure 7). In each case, heptamethines **1-6** featuring *cyanine* characters are bundled together in a narrow region, indicating almost identical electronic structure within this family. On the other hand, strong variations are observed among the *bis-dipole* family, illustrating very important electronic redistribution upon increasing the electron-donating strength of the central substituent. The choice of the Y substituent is thus crucial to control the electronic structure of the polymethines. It is particularly striking that, in addition to the coarse tuning, fine tuning can be also achieved as illustrated by the aniline series **7a-d**, where subtle variations of the electronic density on the nitrogen atom allow progressively moving from a bis-dipolar to a cyanine form.

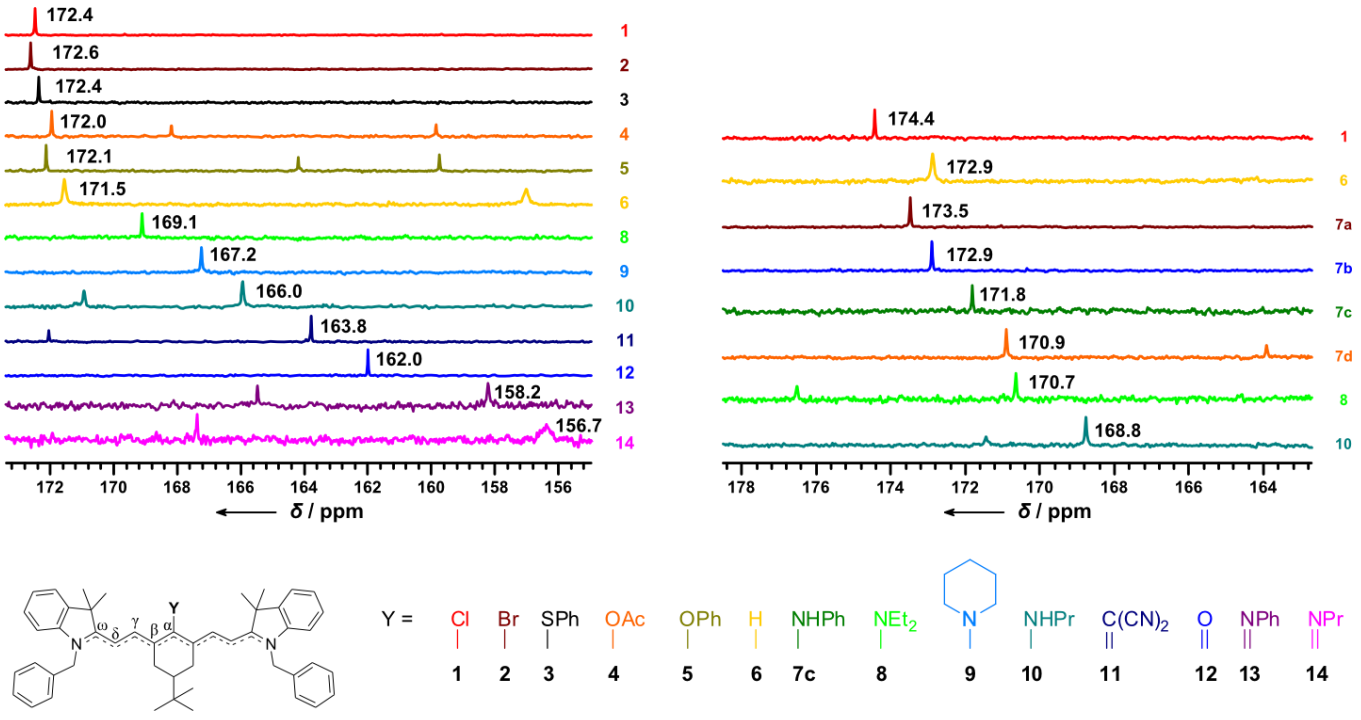

Figure 6. Comparison of ^{13}C NMR spectra in $CDCl_3$ (left) and CD_3OD (right). Indicated chemical shifts are given for Cω carbon atom.

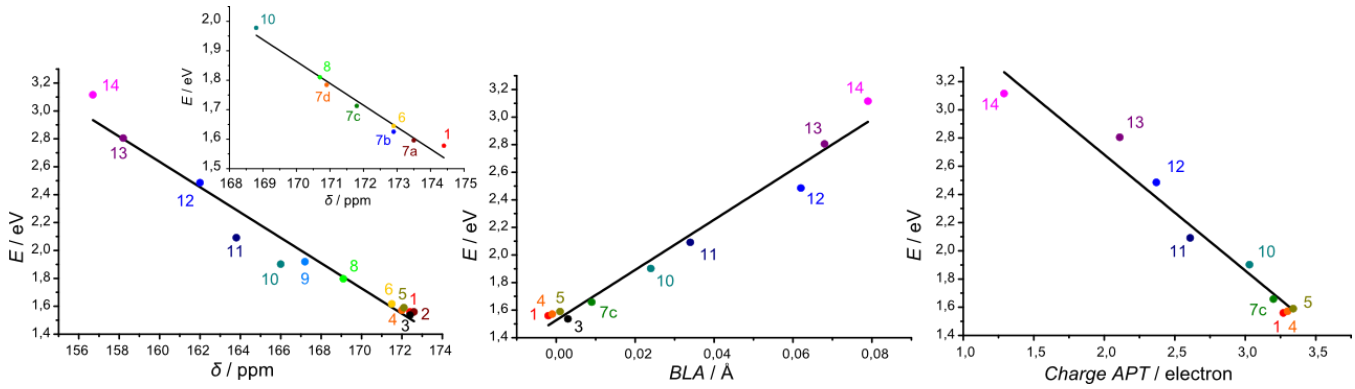

Figure 7. Correlation graphs plotting δ vs. Energy deduced from absorption in DCM (left), BLA vs. Energy (middle) and Cα charge vs. Energy (right). δ vs. Energy deduced from absorption in MeOH (inset).

Conclusion

In conclusion, this study demonstrates the possibility of localizing the cationic charge at the central position of polymethine dyes owing to a rational tuning of the electron-donating ability of the central substituent. The ground-state electronic configuration resulting of this charge localization can be described as a *bis-dipole*, since it presents a charge transfer type transition from the lateral donor groups to the central carbocation, that is blue shifted as compared to that of related *cyanine*. It is possible to tune in both coarse and fine ways the magnitude of this hypsochromic shift by changing the electron-donating strength of the central substituent. This model was validated both experimentally and theoretically, and linear correlations were established between the absorption spectra evolution and parameters relevant for the progressive charge (de)localization over the conjugated backbone (^{13}C NMR chemical shift, BLA extracted from DFT optimized geometries and calculated APT charge).

On a broader perspective, this article proposes a more complete description of the spectral richness of polymethine dyes, nowadays ubiquitous in biology and material science. It constitutes a strong evidence that this class of compound should be depicted not only under two but better under three different ground state electronic configurations depending on the delocalized/localized character of the cationic charge: the *cyanine* with a fully delocalized charge, the *dipole* with a localized charge at one extremity and now the

bis-dipole with the charge localized at the central position. It is possible to favor one or the other configuration by playing with the substitution of the polymethine or by exogenous parameters (solvent, temperature, counter-ion) and we believe that, in the future, the photophysical properties of the polymethine dyes should be rationalized using this three different configurations.

Experimental section

Computational details. All calculations were carried out with the Gaussian09 program[48] tightening both self-consistent field (10^{-10} a.u.) and geometry optimisation (10^{-5} a.u.) convergence thresholds. The calculations were performed on structure in which the two side benzyl groups were replaced by methyl in order to lighten the computational burden. We have applied the default DFT integration grid, namely a pruned (75,302) grid, except when convergence problem appeared and that a tighter pruned (99,590) grid was necessary. For a given heptamethine, the same integration grid was systematically used for all steps of the computational protocol that consists of three successive stages: (1) the ground-state geometrical parameters were calculated at the DFT level, through a force-minimisation process; (2) the vibrational spectrum of each derivatives were determined analytically at the same level of theory and it was checked that all structures correspond to true minima of the potential energy surface; (3) the first five low-lying excited states were calculated within the vertical linear-response TD-DFT approximation.[49, 50] All atoms were described with the split-valence doubly-polarized 6-311G(2d,p) atomic basis set. The solvent effects were accounted for with the polarizable continuum model (PCM),[51] with dichloromethane and methanol as selected solvents. Three functionals, namely M06-2X,[52] PBE0[53, 54] and ωB97X-D[55] were considered. Atomic polar tensor (APT) charges, *i.e.* charges derived from the tensor of the derivatives of dipole moment with respect to atomic cartesian coordinates,[56] were computed during the vibrational frequency calculations. Density difference plots corresponding to the relevant excited-state were computed at the same levels of theory and are represented using a contour threshold of 0.0004 au. In these representations, blue (red) regions indicate loss (gain) of electron density upon transition.

Vibronic spectra were computed on the same structures (but for the replacement of the *t*-Bu group by a methyl) using a PCM-M06-2X/6-31G(d) protocol that has been shown to lead reliable transition energies and band topologies.[57, 58] The vibrationally resolved spectra -within the harmonic approximation- were computed using the FCclasses program.[59, 60] The reported spectra were simulated using a convoluting Gaussian functions presenting a full width at half-maximum (fwhm) of 0.08 eV. A maximal number of 25 overtones for each mode and 20 combination bands on each pair of modes were included in the calculation. The maximum number of integrals to be computed for each class was set to $1x10^8$ or $1x10^{10}$, and it was checked that such number provide converged FC factors (> 0.9).

Synthesis

General Methods. NMR spectra (^1H, ^{13}C) were recorded at room temperature on a BRUKER® Advance operating at 500.10 MHZ and 125.75 MHz for ^1H and ^{13}C, respectively. ^{13}C NMR spectra were recorded using the μDEFT experiment[61] and signals were assigned using HSQC and HMBC experiments. Data are listed in parts per million (ppm) and are reported relative to residual solvent peaks being used as internal standard (^1H ($CDCl_3$): 7.26 ppm, ^{13}C ($CDCl_3$): 77.2 ppm; ^1H (CD_3OD): 3.31 ppm, ^{13}C (CD_3OD): 49.0 ppm). UV-visible spectra were recorded on a Jasco® V-670 spectrophotometer in spectrophotometric grade methanol or dichloromethane solutions (ca. 10^{-5} or 10^{-6} mol L^{-1}). Molar extinction coefficients (ε) were determined at least two times. High resolution mass spectrometry measurements were performed at Centre Commun de Spectrometrie de Masse (Villeurbanne, France). Starting materials were purchased from Sigma Aldrich®, Acros Organics® or Alfa Aesar® with the best available quality grade. All reactions were routinely performed under argon atmosphere in anhydrous solvents. Column chromatography was performed Acros Organics® (0.035-0.070 mm) silicagel. All reagents were purchased from commercial sources and used without further purification, otherwise noted. Syntheses of precursors and of compounds **1**, **3**, **5**, **8**, **9**, **10** directly adapted from literature procedures are reported in SI.

2. To a solution of 100 mg of 5-tert-butyl-2-bromo-3-hydroxymethylene-cyclohex-1-enecarbaldehyde (0.37 mmol, 1 eq.) and 277 mg indolium salt (0.81 mmol, 2.2 eq.) in 8 mL of absolute ethanol were added 0.07 mL of pyridine (0.92 mmol, 2.5 eq.). The solution was stirred for 18h at 40°C. The resulting green solution was concentrated, dissolved in DCM, washed with an aqueous solution of HBr 1M and an aqueous saturated $NaHCO_3$ solution. The organic layer was dried over Na_2SO_4, filtered and concentrated. The crude was purified by flash chromatography on silica with DCM/methanol as eluent (98:2, $R_f = 0.18$) and finally precipitated in Et_2O to afford cyanine **2** as a green solid in a 55 % yield (165 mg). ^{1}H NMR ($CDCl_3$, 500.10 MHz): δ 8.25 (d, ^3J = 14 Hz, 2H), 7.43-7.24 (m, 18H), 6.22 (d, ^3J = 14 Hz, 2H), 5.54 (d, ^2J = 16.5 Hz, 2H), 5.45 (d, ^2J = 16.5 Hz, 2H), 2.64 (d, ^2J = 15 Hz, 2H), 2.09 (dd, ^2J = 14 Hz, ^3J = 13 Hz, 2H), 1.77 (s, 6H), 1.75 (s, 6H), 1.39 (m, 1H), 0.99 (s, 9H). ^{13}C NMR ($CDCl_3$, 125.75 MHz): δ 172.6, 147.5, 146.7, 143.0, 141.1, 134.6, 130.7, 129.4, 129.1, 128.4, 126.8, 125.6, 122.5, 111.3, 103.1, 49.5, 48.7, 42.3, 32.5, 28.7, 28.3, 28.2, 27.6. UV-Vis (CH_3OH) λ_{max} = 787 nm (ε_{max} = 297 000 L.mol^{-1}.cm^{-1}). UV-Vis (DCM) λ_{max} = 795 nm (ε_{max} = 376000 L.mol^{-1}.cm^{-1}). HRMS (ESI+): $[M]^+$ = 735.3325 (calcd for $C_{48}H_{52}BrN_2$: 735.3308).

4. To a solution of 65 mg of ketocyanine **12** (0.10 mmol, 1 eq.) in 5 mL of anhydrous DCM were added dropwise 0.07 mL of acetyl chloride (0.96 mmol, 10 eq.) at 0°C. The mixture was stirred for 15 minutes at this temperature, then allowed to warm to RT and finally quenched with one drop of distilled DIEA. The crude mixture was washed with an aqueous saturated NaCl solution; the organic layer was dried over Na_2SO_4, filtered and concentrated. Flash column chromatography on silica using DCM/MeOH as eluent (95:5, $R_f = 0.19$) permit to afford compound **4** as a green solid in a 49 % yield (34 mg). ^{1}H NMR ($CDCl_3$, 500.10 MHz): δ 7.59 (d, $^3J_{trans}$ = 14 Hz, 2H), 7.40-7.38 (m, 2H), 7.38-7.30 (m, 8H), 7.29-7.22 (m, 6H), 7.18-7.17 (m, 2H), 6.06 (d, $^3J_{trans}$ = 14 Hz, 2H), 5.37 (m, 4H), 2.57 (d, ^2J = 15 Hz, 2H), 2.39 (s, 3H), 2.01 (dd, ^2J = 14 Hz, ^3J = 14 Hz, 2H), 1.68 (s, 6H), 1.65 (s, 6H), 1.47 (m, 1H), 0.97 (s, 9H). ^{13}C NMR ($CDCl_3$, 125.75 MHz): δ 171.9, 168.2, 159.8, 142.9, 140.7, 140.2, 134.4, 129.5, 129.2, 128.6, 126.8, 125.6, 123.7, 122.5, 111.2, 101.8, 49.3, 48.6, 42.2, 32.6, 28.5, 28.4, 27.6, 25.5, 20.8. UV-Vis (CH_3OH) λ_{max} = 780 nm

(ε_{max} = 257000 L.mol^{-1}.cm^{-1}).UV-Vis (DCM) λ_{max} = 789 nm (ε_{max} = 273000 L.mol^{-1}.cm^{-1}). HRMS (ESI+): $[M]^+$ = 715.4253 (calcd for $C_{50}H_{55}N_2O_2$: 715.4258).

6. 50 mg of cyanine **2** (0.06 mmol, 1 eq.), 103 mg of sodium ethanethiolate (1.22 mmol, 20 eq.) and 0.10 mL of ethanethiol (1.35 mmol, 22 eq.) were dissolved in 2 mL of anhydrous DMF and stirred for 2 hours at 100°C. The reaction mixture was allowed to cool to RT, added by DCM, washed with water and an aqueous solution of HBr 1M. The organic layer was dried over Na_2SO_4 and finally concentrated. The crude residue was purified by flash chromatography on silica DCM/MeOH (90/10, R_f = 0.44) to afford **6** as a green solid in a 47% yield (21 mg). ^{1}H NMR ($CDCl_3$, 500.10 MHz): δ 7.74 (d, ^{3}J = 13 Hz, 2H), 7.59 (s, 1H), 7.39-7.27 (m, 14H), 7.21 (t, ^{3}J = 7 Hz, 2H), 7.10 (d, ^{3}J = 7 Hz, 2H), 5.99 (d, ^{3}J = 13 Hz, 2H), 5.27 (m, 4H), 2.44 (d, ^{2}J = 14 Hz, 2H), 1.84 (dd, ^{2}J = 13 Hz, ^{3}J = 13 Hz, 2H), 1.78 (s, 6H), 1.76 (s, 6H), 1.36 (m, 1H), 0.95 (s, 9H). ^{13}C NMR ($CDCl_3$, 125.75 MHz): δ 171.5, 157.1, 149.0, 142.9, 141.0, 134.5, 134.1, 129.4, 128.8, 128.4, 126.7, 125.0, 122.6, 110.4, 100.7, 49.3, 48.1, 43.0, 32.6, 28.3, 28.2, 27.6, 25.2. UV-Vis (CH_3OH) λ_{max} = 754 nm (ε_{max} = 234 000 L.mol^{-1}.cm^{-1}). UV-Vis (DCM) λ_{max} = 767 nm (ε_{max} = 268000 L.mol^{-1}.cm^{-1}). HRMS (ESI+): $[M]^+$ = 657.4189 (calcd for $C_{48}H_{53}N_2$: 657.4203).

7a. A solution of 100 mg of cyanine **1** (129 µmol, 1 eq.) and 120 mg of 4-nitroaniline (903 µmol, 7 eq.) in 2 mL of anhydrous DMF was stirred for 8h at 130°C under micro-wave irradiation. The reaction mixture was allowed to cool to RT and was extracted with DCM. The resulting organic phase was washed three times with an aqueous HBr 1M solution, dried over Na_2SO_4 and evaporated. The crude residue was purified by flash column chromatography on silica with DCM/MeOH (from 97:3 to 95:5) as eluent to afford **7a** as a dark blue solid (40 mg, 35%).^{1}H NMR (CD_3OD, 500.10 MHz): δ 8.11 (d, ^{3}J = 8 Hz, 2H), 7.94 (d, ^{3}J = 14 Hz, 2H), 7.42 (d, ^{3}J = 7 Hz, 2H), 7.36-7.21 (m, 16H), 6.84 (d, ^{3}J = 7 Hz, 2H), 6.11 (d, ^{3}J = 13 Hz, 2H), 5.36 (d, ^{2}J = 16 Hz, 2H), 5.31 (d, ^{2}J = 16 Hz, 2H), 2.66 (d, ^{2}J = 14 Hz, 2H), 1.97 (dd, ^{2}J = 13 Hz, ^{3}J = 13 Hz, 2H), 1.41 (s, 6H), 1.40 (s, 6H), 1.31 (m, 1H), 0.99 (s, 9H).^{13}C NMR (CD_3OD, 125.75 MHz): δ 173.5, 156.0, 154.7, 144.3, 144.0, 142.2, 140.6, 136.3, 130.3, 129.9, 129.2, 128.5, 127.7, 127.4, 126.2, 123.6, 115.0,

111.8, 102.1, 50.1, 48.4, 44.4, 33.4, 28.3, 28.3, 27.7, 26.9.UV-Vis (CH_3OH) λ_{max} = 777 nm (ε_{max} = 235000 $L.mol^{-1}.cm^{-1}$). HRMS (ESI+): $[M]^+$ = 793.4460 (calcd for $C_{54}H_{57}N_4O_2$: 793.4476).

7b. A solution of 100 mg of cyanine **1** (129 µmol, 1 eq.) and 81 µL of 4-trifluoromethylaniline (647 µmol, 5 eq.) in 2 mL of anhydrous DMF was stirred for 4h at 100°C under micro-wave irradiation. The reaction mixture was allowed to cool to RT and was extracteed with DCM. The resulting organic phase was washed twice with an aqueous HBr 1M solution, dried over Na_2SO_4 and evaporated. The crude residue was purified by flash column chromatography on silica with DCM/MeOH (from 97:3 to 95:5) as eluent to afford compound **7b** as a dark blue solid (60 mg, 52%). ^1H NMR (CD_3OD, 500.10 MHz): δ 7.98 (d, ^3J = 14 Hz, 2H), 7.50 (d, ^3J = 8 Hz, 2H), 7.42 (d, ^3J = 7 Hz, 2H), 7.37-7.19 (m, 16H), 6.98 (d, ^3J = 8 Hz, 2H), 6.02 (d, ^3J = 14 Hz, 2H, 5.31 (s, 4H), 2.62 (d, ^2J = 15 Hz, 2H), 1.91 (dd, ^2J = 14 Hz, ^3J = 14 Hz, 2H), 1.40 (s, 6H), 1.39 (s, 6H), 1.29 (m, 1H), 0.97 (s, 9H). ^{13}C NMR (CD_3OD, 125.75 MHz): δ 172.9, 158.8, 151.4, 144.4, 144.2, 142.0, 136.4, 130.2, 129.8, 129.3, 129.1, 128.2, 128.2, 127.6, 127.2, 125.8, 123.5, 117.0, 111.4, 101.1, 49.9, 48.4, 44.7, 33.4, 28.4, 28.4, 27.7, 26.9. UV-Vis (CH_3OH) λ_{max} = 763 nm (ε_{max} = 183000 $L.mol^{-1}.cm^{-1}$). HRMS (ESI+): $[M]^+$ = 816.4474 (calcd for $C_{55}H_{57}F_3N_3$: 816.4499).

7c. A solution of 200 mg of cyanine **1** (0.26 mmol, 1 eq.) and 94 µL of distilled aniline (1.04 mmol, 4 eq.) in 3 mL of anhydrous DMF was stirred for 8h at 70°C. The reaction mixture was allowed to cool to RT and was extracted with DCM. The resulting organic phase was washed three times with an aqueous HBr 1M solution, dried over Na_2SO_4 and concentrated. The crude residue was purified by flash chromatography on silica with EtOAc/DCM/MeOH (from 50:50:0 to 45:45:10) as eluent to afford **7c** as a dark blue solid in a 84% yield (180 mg). ^1H NMR (CD_3OD, 500.10 MHz): δ 7.99 (d, ^3J = 14 Hz, 2H), 7.38 (d, ^3J = 7 Hz, 2H), 7.34-7.27 (m, 9H), 7.24-7.14 (m, 9H), 7.03 (d, ^3J = 8 Hz, 2H), 6.87 (t, ^3J = 7 Hz, 1H), 5.89 (d, ^3J = 14 Hz, 2H), 5.26 (d, ^2J = 17 Hz, 2H), 5.22 (d, ^2J = 17 Hz, 2H), 2.57 (dd, ^2J = 12 Hz, ^3J = 3 Hz, 2H), 1.82 (dd, ^2J = 13 Hz, ^3J = 13 Hz, 2H), 1.40 (s, 6H), 1.38 (s, 6H), 1.33 (m, 1H), 0.92 (s, 9H). ^{13}C NMR (CD_3OD, 125.75 MHz): δ 171.8, 162.3, 147.2, 144.6, 143.9, 141.8, 136.5, 131.1, 130.2, 129.9, 129.7, 129.0, 127.6, 125.2,

123.4, 122.9, 119.6, 110.9, 99.7, 49.6, 48.2, 45.1, 33.4, 28.6, 28.6, 27.6, 27.0. UV-Vis (CH_3OH) λ_{max} = 724 nm (ε_{max} = 129000 $L.mol^{-1}.cm^{-1}$). HRMS (ESI+): $[M]^+$ = 748.4625 (calcd for $C_{54}H_{58}N_3$: 748.4625).

7d. A solution of 100 mg of cyanine **1** (0.13 mmol, 1 eq.) and 64 mg of *p*-anisidine (0.52 mmol, 4 eq.) in 2 mL of anhydrous DMF was stirred for 1h at 80°C. The reaction mixture was allowed to cool to RT and DMF was evaporated. Then DCM was added and the organic layer was washed with an aqueous HBr 1M solution and water, dried over Na_2SO_4 and concentrated. The crude residue was purified by flash chromatography on silica with DCM/MeOH (95:5, R_f = 0.56) as eluent and precipitated in pentane to afford compound **7d** as a dark blue solid in a 87% yield (97 mg). ^{1}H NMR (CD_3OD, 500.10 MHz): δ 7.93 (d, ^3J = 13 Hz, 2H), 7.36-7.06 (m, 20H), 6.90 (d, ^3J = 7 Hz, 2H), 5.79 (d, ^3J = 13 Hz, 2H), 5.22 (d, ^2J = 17 Hz, 2H), 5.16 (d, ^2J = 17 Hz, 2H), 3.74 (s, 3H), 2.51 (d, ^2J = 13 Hz, 2H), 1.76 (dd, ^2J = 13 Hz, ^3J = 13 Hz, 2H), 1.41 (s, 6H), 1.38 (s, 6H), 1.26 (m, 1H), 0.87 (s, 9H). ^{13}C NMR (CD_3OD, 125.75 MHz): δ 170.9, 163.9, 157.2, 144.8, 143.1, 141.5, 139.7, 136.6, 130.2, 129.6, 128.9, 127.5, 124.9, 123.3, 122.5, 116.6, 110.6, 98.7, 56.1, 48.8, 48.0, 45.3, 33.4, 28.7, 28.6, 27.6, 27.1 1 C_{quat} is missing. UV-Vis (CH_3OH) λ_{max} = 695 nm (ε_{max} = 107000 $L.mol^{-1}.cm^{-1}$). HRMS (ESI+): $[M]^+$ = 778.4714 (calcd for $C_{55}H_{60}N_3O$: 778.4731).

11. A solution of 30 mg of cyanine **1** (0.04 mmol, 1 eq.) and 3.8 mg of malononitrile (0.06 mmol, 1.5 eq.) in 2 mL of anhydrous DMF was added by 0.01 mL of distilled DIEA (0.08 mmol, 2 eq.) and the mixture was stirred for 15min at RT. Then DCM was added to the solution. The organic layer was washed with an aqueous saturated solution of NH_4Cl, dried over Na_2SO_4 and concentrated. A purification by flash column chromatography on silica with DCM/MeOH (98:2, R_f = 0.83) affords compound **11** as a blue solid in a 54% yield (15 mg). ^{1}H NMR ($CDCl_3$, 500.10 MHz): δ 7.63 (d, $^3J_{trans}$ = 13 Hz, 2H), 7.33- 7.26 (m, 6H), 7.23-7.20 (m, 4H), 7.00 (t, ^3J = 7 Hz, 2H), 6.81 (d, ^3J = 8 Hz, 2H), 5.46 (d, $^3J_{trans}$ = 13 Hz, 2H), 4.95 (d, ^2J = 17 Hz, 2H), 4.87 (d, ^2J = 17 Hz, 2H), 2.33 (dd, ^2J = 15 Hz, ^3J = 4 Hz, 2H), 1.74 (s, 6H), 1.67 (s, 6H), 1.65 (m, 2H), 1.24 (m, 1H), 0.76 (s, 9H). ^{13}C NMR ($CDCl_3$, 125.75 MHz): δ 172.0, 163.8, 144.3, 140.4, 135.8, 134.4, 129.2, 128.1, 127.8, 127.3, 126.5, 122.3, 121.7, 120.4, 107.5, 94.8, 57.7, 47.1, 46.9, 43.5, 32.7, 30.1,

29.5, 27.4, 27.2. UV-Vis (CH_3OH) λ_{max} = 630 nm (ε_{max} = 75600 $L.mol^{-1}.cm^{-1}$). UV-Vis (DCM) λ_{max} = 593 nm (ε_{max} = 67000 $L.mol^{-1}.cm^{-1}$). HRMS (ESI+): $[M+H]^+$ = 721.4241 (calcd for $C_{51}H_{53}N_4$: 721.4265).

12. To a solution of 40 mg of cyanine **1** (0.05 mmol, 1 eq.) and 12 mg of *N*-hydroxysuccinimide (0.10 mmol, 2 eq.) in 5 mL of anhydrous DMF were added 0.02 mL of distilled DIEA (0.10 mmol, 2 eq.) and the mixture was stirred for 2h at RT. Then 10 mL of DCM were added to the solution. The organic layer was washed with an aqueous saturated solution of NH_4Cl (10 mL) and water (10 mL), dried over Na_2SO_4 and concentrated. After filtration through an activated alumina plug (25 g Al_2O_3 with 6% H_2O) with DCM/petroleum ether (1:1, R_f = 0.26), compound **12** was isolated as a red solid in a 86% yield (30 mg). ^1H NMR ($CDCl_3$, 500.10 MHz): δ 8.04 (d, ^3J = 13 Hz, 2H), 7.33-7.30 (m, 4H), 7.27-7.22 (m, 8H), 7.17 (t, ^3J = 8 Hz, 2H), 6.94 (t, ^3J = 7 Hz, 2H), 6.72 (d, ^3J = 8 Hz, 2H), 5.42 (d, ^3J = 13 Hz, 2H), 4.91 (d, ^2J = 16 Hz, 2H), 4.84 (d, ^2J = 16 Hz, 2H), 2.57 (dd, ^2J = 15 Hz, ^3J = 3 Hz, 2H), 1.88 (dd, ^2J = 14 Hz, ^3J = 14 Hz, 2H), 1.70 (s, 12H), 1.34 (m, 1H), 0.90 (s, 9H). ^{13}C NMR ($CDCl_3$, 125.75 MHz): δ 186.7, 162.0, 144.8, 139.6, 136.4, 132.4, 129.0, 127.9, 127.6, 127.5, 126.7, 122.0, 120.8, 106.8, 94.0, 46.7, 46.6, 43.3, 32.6, 28.9, 28.9, 27.5, 26.7. UV-Vis (CH_3OH) λ_{max} = 526 nm (ε_{max} = 50000 $L.mol^{-1}.cm^{-1}$). UV-Vis (DCM) λ_{max} = 499 nm (ε_{max} = 40000 $L.mol^{-1}.cm^{-1}$). HRMS (ESI+): $[M+H]^+$ = 673.4120 (calcd for $C_{48}H_{53}N_2O$: 673.4152).

13. Compound **13** was quantitatively formed by treatment of a solution of compound **7c** in DCM or $CDCl_3$ with an aqueous K_2CO_3 solution (1M). Analyses were performed in situ. ^1H NMR ($CDCl_3$, 500.10 MHz): δ 7.28-7.19 (m, 18H), 6.87-6.80 (m, 5H), 6.62 (d, ^3J = 8 Hz, 2H), 5.23 (d, ^3J = 12 Hz, 2H), 4.77 (m, 4H), 2.45 (d, ^2J = 12 Hz, 2H), 1.83 (dd, ^2J = 14 Hz, ^3J = 14 Hz, 2H), 1.40-1.29 (m, 13H), 0.84 (s, 9H). ^{13}C NMR ($CDCl_3$, 125.75 MHz): δ 165.5, 158.2, 154.4, 145.2, 139.3, 136.8, 133.6, 129.5, 128.9, 127.8, 127.4, 126.7, 121.9, 120.9, 120.1, 120.0, 106.1, 93.8, 46.5, 45.6, 43.7, 32.7, 28.7, 28.5, 27.8, 27.4 (1 CH is missing). UV-Vis (DCM) λ_{max} = 442 nm (ε_{max} = 50000 $L.mol^{-1}.cm^{-1}$).

14. Compound **14** was quantitatively formed by treatment of compound **10** in DCM or $CDCl_3$ with an aqueous K_2CO_3 solution (1M). Analyses were performed in situ. ^1H NMR ($CDCl_3$, 500.10 MHz): δ 7.29-7.21 (m, 12H), 7.17-7.11 (m, 4H), 6.84 (t, 2H, ^3J = 7 Hz), 6.63 (d, 2H, ^3J = 8 Hz), 5.25 (d, ^3J = 12 Hz, 2H),

4.78 (m, 4H), 3.56 (t, 2H, ^{3}J = 7 Hz), 2.41-2.38 (m, 2H), 1.82-1.78 (m, 2H), 1.70 (m, 2H), 1.62 (bs, 6H), 1.59 (bs, 6H), 1.31 (m, 1H), 1.02 (t, ^{3}J = 7 Hz, 3H), 0.81 (s, 9H). ^{13}C NMR ($CDCl_3$, 125.75 MHz): δ 167.5, 156.5, 145.5, 139.1, 137.0, 128.9 (HSQC showed that 2 carbons have this *δ*), 127.8, 127.4, 126.7, 121.9, 119.7, 106.0, 94.4, 55.5, 46.6, 45.5, 43.7, 32.6, 28.7, 27.4, 25.9, 12.3. (1 C_{quat} is missing) UV-Vis (DCM) λ_{max} = 398 nm (ε_{max} = 44000 $L.mol^{-1}.cm^{-1}$).

Acknowledgements

A.C.E. thanks the European Research Council (ERC, Marches 278845) for his post-doctoral grant. D.J. acknowledges the European Research Council (ERC) and the Région des Pays de la Loire for financial support in the framework of a Starting Grant (Marches - 278845) and a recrutement sur poste stratégique, respectively. This research used resources of 1) the GENCI-CINES/IDRIS (Grant c2012085117), 2) CCIPL (Centre de Calcul Intensif des Pays de Loire), 3) a local Troy cluster.

Supporting Information Available

Full width at half-maximum extracted from absorption spectra, solvatochromism experiments, additional theoretical data, concentration-dependent absorption study, synthesis details and complete characterizations including NMR spectra of all compounds are provided. This material is available free of charge via the internet at https://pubs.acs.org/doi/10.1021/jp501358q.

References

1. Fabian, J.; Nakazumi, H.; Matsuoka, M., Near-infrared Absorbing Dyes. *Chem. Rev.* **1992,** *92*, 1197-1226.
2. Mishra, A.; Behera, R. K.; Behera, P. K.; Mishra, B. K.; Behera, G. B., Cyanines During the 1990s: A Review. *Chem. Rev.* **2000,** *100*, 1973-2012.
3. Frangioni, J. V., In Vivo Near-Infrared Fluorescence Imaging. *Curr. Op. Chem. Biol.* **2003,** *7*, 626-634.
4. Kiyose, K.; Kojima, H.; Nagano, T., Functional Near-Infrared Fluorescent Probes. *Chem. Asian J.* **2008,** *3*, 506-515.

5. Przhonska, O.; Webster, S.; Padilha, L.; Hu, H.; Kachkovski, A.; Hagan, D.; Stryland, E., Two-Photon Absorption in Near-IR Conjugated Molecules: Design Strategy and Structure–Property Relations. In *Advanced Fluorescence Reporters in Chemistry and Biology I*, Demchenko, A. P., Ed. Springer Berlin Heidelberg: 2010; Vol. 8, pp 105-147.
6. Hu, C.; Sun, W.; Cao, J.; Gao, P.; Wang, J.; Fan, J.; Song, F.; Sun, S.; Peng, X., A Ratiometric Near-Infrared Fluorescent Probe for Hydrazine and Its in Vivo Applications. *Org. Lett.* **2013,** *15*, 4022-4025.
7. Wang, X.; Sun, J.; Zhang, W.; Ma, X.; Lv, J.; Tang, B., A Near-infrared Ratiometric Fluorescent Probe For Rapid and Highly Sensitive Imaging of Endogenous Hydrogen Sulfide in Living Cells. *Chem. Sci.* **2013,** *4*, 2551-2556.
8. Hales, J. M.; Matichak, J.; Barlow, S.; Ohira, S.; Yesudas, K.; Brédas, J.-L.; Perry, J. W.; Marder, S. R., Design of Polymethine Dyes with Large Third-Order Optical Nonlinearities and Loss Figures of Merit. *Science* **2010,** *327*, 1485-1488.
9. Bellier, Q.; Makarov, N. S.; Bouit, P.-A.; Rigaut, S.; Kamada, K.; Feneyrou, P.; Berginc, G.; Maury, O.; Perry, J. W.; Andraud, C., Excited State Absorption: a Key Phenomenon for the Improvement of Biphotonic Based Optical Limiting at Telecommunication Wavelengths. *Phys. Chem. Chem. Phys.* **2012,** *14*, 15299-15307.
10. Bouit, P.-A.; Di Piazza, E.; Rigaut, S.; Le Guennic, B.; Aronica, C.; Toupet, L.; Andraud, C.; Maury, O., Stable Near-Infrared Anionic Polymethine Dyes: Structure, Photophysical, and Redox Properties. *Org. Lett.* **2008,** *10*, 4159-4162.
11. Terenziani, F.; Painelli, A.; Katan, C.; Charlot, M.; Blanchard-Desce, M., Charge Instability in Quadrupolar Chromophores: Symmetry Breaking and Solvatochromism. *J. Am. Chem. Soc.* **2006,** *128*, 15742-15755.
12. Terenziani, F.; Przhonska, O. V.; Webster, S.; Padilha, L. A.; Slominsky, Y. L.; Davydenko, I. G.; Gerasov, A. O.; Kovtun, Y. P.; Shandura, M. P.; Kachkovski, A. D.; Hagan, D. J.; Van Stryland, E. W.; Painelli, A., Essential-State Model for Polymethine Dyes: Symmetry Breaking and Optical Spectra. *J. Phys. Chem. Lett.* **2010,** *1*, 1800-1804.
13. Dähne, S.; Radeglia, R., Revision der Lewis-Calvin-Regel zur Charakterisierung Vinyloger Polyen- und Polymethinähnlicher Verbindungen. *Tetrahedron* **1971,** *27*, 3673-3693.
14. Dähne, S., Color and Constitution: One Hundred Years of Research. *Science* **1978,** *199*, 1163-1167.
15. Marder, S. R.; Gorman, C. B.; Tiemann, B. G.; Perry, J. W.; Bourhill, G.; Mansour, K., Relation Between Bond-Length Alternation and Second Electronic Hyperpolarizability of Conjugated Organic Molecules. *Science* **1993,** *261*, 186-189.
16. Brooker, L. G. S.; Sprague, R. H.; Smyth, C. P.; Lewis, G. L., Color and Constitution. I. Halochromism of Anhydronium Bases Related to the Cyanine Dyes 1. *J. Am. Chem. Soc.* **1940,** *62*, 1116-1125.
17. Tolbert, L. M.; Zhao, X., Beyond the Cyanine Limit: Peierls Distortion and Symmetry Collapse in a Polymethine Dye. *J. Am. Chem. Soc.* **1997,** *119*, 3253-3258.
18. Lepkowicz, R. S.; Przhonska, O. V.; Hales, J. M.; Fu, J.; Hagan, D. J.; Van Stryland, E. W.; Bondar, M. V.; Slominsky, Y. L.; Kachkovski, A. D., Nature of the Electronic Transitions in Thiacarbocyanines With a Long Polymethine Chain. *Chem. Phys.* **2004,** *305*, 259-270.
19. Hu, H.; Przhonska, O. V.; Terenziani, F.; Painelli, A.; Fishman, D.; Ensley, T. R.; Reichert, M.; Webster, S.; Bricks, J. L.; Kachkovski, A. D.; Hagan, D. J.; Van Stryland, E. W., Two-Photon Absorption Spectra of a Near-Infrared 2-azaazulene Polymethine Dye: Solvation and Ground-State Symmetry Breaking. *Phys. Chem. Chem. Phys.* **2013,** *15*, 7666-7678.
20. Bouit, P.-A.; Aronica, C.; Toupet, L.; Le Guennic, B.; Andraud, C.; Maury, O., Continuous Symmetry Breaking Induced by Ion Pairing Effect in Heptamethine Cyanine Dyes: Beyond the Cyanine Limit. *J. Am. Chem. Soc.* **2010,** *132*, 4328-4335.
21. Pascal, S.; Bouit, P.-A.; Le Guennic, B.; Parola, S.; Maury, O.; Andraud, C., Symmetry Loss of Heptamethine Cyanines: an Example of Dipole Generation by Ion-pairing Effect. *Proc. SPIE* **2013**, 8622, 86220F.

22. Würthner, F.; Archetti, G.; Schmidt, R.; Kuball, H.-G., Solvent Effect on Color, Band Shape, and Charge-Density Distribution for Merocyanine Dyes Close to the Cyanine Limit. *Angew. Chem. Int. Ed.* **2008,** *47*, 4529-4532.
23. Rettig, W.; Dekhtyar, M., Merocyanines: Polyene–Polymethine Transition in Donor–Acceptor-Substituted Stilbenes and Polyenes. *Chem. Phys.* **2003,** *293*, 75-90.
24. Mustroph, H.; Mistol, J.; Senns, B.; Keil, D.; Findeisen, M.; Hennig, L., Relationship between the Molecular Structure of Merocyanine Dyes and the Vibrational Fine Structure of Their Electronic Absorption Spectra. *Angew. Chem. Int. Ed.* **2009,** *48*, 8773-8775.
25. Since the structures are formally non-centrosymmetric, the denomination quadrupole cannot be applied.
26. Sissa, C.; Terenziani, F.; Painelli, A.; Siram, R. B. K.; Patil, S., Spectroscopic Characterization and Modeling of Quadrupolar Charge-Transfer Dyes with Bulky Substituents. *J. Phys. Chem. B* **2012,** *116*, 4959-4966.
27. Zou, Q.; Zhao, Y.; Makarov, N. S.; Campo, J.; Yuan, H.; Fang, D.-C.; Perry, J. W.; Wu, F., Effect of Alicyclic Ring Size on the Photophysical and Photochemical Properties of Bis(arylidene)cycloalkanone Compounds. *Phys. Chem. Chem. Phys.* **2012,** *14*, 11743-11752.
28. Strekowski, L.; Lipowska, M.; Patonay, G., Substitution Reactions of a Nucleofugal Group in Heptamethine Cyanine Dyes. Synthesis of an Isothiocyanato Derivative for Labeling of Proteins With a Near-Infrared Chromophore. *J. Org. Chem.* **1992,** *57*, 4578-4580.
29. Reynolds, G. A.; Drexhage, K. H., Stable Heptamethine Pyrylium Dyes That Absorb in the Infrared. *J. Org. Chem.* **1977,** *42*, 885-888.
30. L. Gallaher, J. D.; E. Johnson, M., Development of Near-Infrared Fluorophoric Labels for the Determination of Fatty Acids Separated by Capillary Electrophoresis With Diode Laser Induced Fluorescence Detection. *Analyst* **1999,** *124*, 1541-1546.
31. Flanagan, J. H.; Khan, S. H.; Menchen, S.; Soper, S. A.; Hammer, R. P., Functionalized Tricarbocyanine Dyes as Near-Infrared Fluorescent Probes for Biomolecules. *Bioconjugate Chem.* **1997,** *8*, 751-756.
32. Bouit, P.-A.; Spänig, F.; Kuzmanich, G.; Krokos, E.; Oelsner, C.; Garcia-Garibay, M. A.; Delgado, J. L.; Martín, N.; Guldi, D. M., Efficient Utilization of Higher-Lying Excited States to Trigger Charge-Transfer Events. *Chem. Eur. J.* **2010,** *16*, 9638-9645.
33. Peng, X.; Song, F.; Lu, E.; Wang, Y.; Zhou, W.; Fan, J.; Gao, Y., Heptamethine Cyanine Dyes with a Large Stokes Shift and Strong Fluorescence: A Paradigm for Excited-State Intramolecular Charge Transfer. *J. Am. Chem. Soc.* **2005,** *127*, 4170-4171.
34. Kiyose, K.; Aizawa, S.; Sasaki, E.; Kojima, H.; Hanaoka, K.; Terai, T.; Urano, Y.; Nagano, T., Molecular Design Strategies for Near-Infrared Ratiometric Fluorescent Probes Based on the Unique Spectral Properties of Aminocyanines. *Chem. Eur. J.* **2009,** *15*, 9191-9200.
35. Strekowski, L.; Mason, J. C.; Say, M.; Lee, H.; Gupta, R.; Hojjat, M., Novel Synthetic Route to pH-Sensitive 2,6-bis(substituted ethylidene)cyclohexanone/hydroxycyanine Dyes that Absorb in the Visible/Near-Infrared Regions. *Heterocycl. Commun.* **2005,** *11*, 129-134.
36. Mayerhöffer, U.; Gsänger, M.; Stolte, M.; Fimmel, B.; Würthner, F., Synthesis and Molecular Properties of Acceptor-Substituted Squaraine Dyes. *Chem. Eur. J.* **2013,** *19*, 218-232.
37. Matichak, J. D.; Hales, J. M.; Barlow, S.; Perry, J. W.; Marder, S. R., Dioxaborine- and Indole-Terminated Polymethines: Effects of Bridge Substitution on Absorption Spectra and Third-Order Polarizabilities. *J. Phys. Chem. A* **2011,** *115*, 2160-2168.
38. Fabian, J., Symmetry-Lowering Distortion of Near-Infrared Polymethine Dyes—a Study by First-Principles Methods. *J. Mol. Struct. THEOCHEM* **2006,** *766*, 49-60.
39. Masunov, A.; Tretiak, S., Prediction of Two-Photon Absorption Properties for Organic Chromophores Using Time-Dependent Density-Functional Theory. *J. Phys. Chem. B* **2003,** *108*, 899-907.

40. Mukhopadhyay, S.; Risko, C.; Marder, S. R.; Bredas, J.-L., Polymethine Dyes for All-Optical Switching Applications: a Quantum-Chemical Characterization of Counter-Ion and Aggregation Effects on the Third-Order Nonlinear Optical Response. *Chem. Sci.* **2012,** *3*, 3103-3112.
41. Karton-Lifshin, N.; Albertazzi, L.; Bendikov, M.; Baran, P. S.; Shabat, D., "Donor–Two-Acceptor" Dye Design: A Distinct Gateway to NIR Fluorescence. *J. Am. Chem. Soc.* **2012,** *134*, 20412-20420.
42. Yesudas, K., Cationic Cyanine Dyes: Impact of Symmetry-Breaking on Optical Absorption and Third-Order Polarizabilities. *Phys. Chem. Chem. Phys.* **2013,** *15*, 19465-19477.
43. Thorley, K. J.; Hales, J. M.; Kim, H.; Ohira, S.; Brédas, J.-L.; Perry, J. W.; Anderson, H. L., Cyanine-Like Dyes with Large Bond-Length Alternation. *Chem. Eur. J.* **2013,** *19*, 10370-10377.
44. Champagne, B.; Guillaume, M.; Zutterman, F., TDDFT Investigation of the Optical Properties of Cyanine Dyes. *Chem. Phys. Lett.* **2006,** *425*, 105-109.
45. Guillaume, M.; Liégeois, V.; Champagne, B.; Zutterman, F., Time-Dependent Density Functional Theory Investigation of the Absorption and Emission Spectra of a Cyanine Dye. *Chem. Phys. Lett.* **2007,** *446*, 165-169.
46. Jacquemin, D.; Zhao, Y.; Valero, R.; Adamo, C.; Ciofini, I.; Truhlar, D. G., Verdict: Time-Dependent Density Functional Theory "Not Guilty" of Large Errors for Cyanines. *J. Chem. Theory Comput.* **2012,** *8*, 1255-1259.
47. The Cω atom is localized far away from the Y substituent and therefore variable inductive effects due to the Y substituent on its chemical shift can be neglected. For all compounds, the corresponding signal was unambiguously assigned by 2D HMBC and HSQC experiments.
48. Frisch, M. J.; Trucks, G. W.; Schlegel, H. B.; Scuseria, G. E.; Robb, M. A.; Cheeseman, J. R.; Scalmani, G.; Barone, V.; Mennucci, B.; Petersson, G. A.; Nakatsuji, H.; Caricato, M.; Li, X.; Hratchian, H. P.; Izmaylov, A. F.; Bloino, J.; Zheng, G.; Sonnenberg, J. L.; Hada, M.; Ehara, M.; Toyota, K.; Fukuda, R.; Hasegawa, J.; Ishida, M.; Nakajima, T.; Honda, Y.; Kitao, O.; Nakai, H.; Vreven, T.; Montgomery, Jr., J. A.; Peralta, J. E.; Ogliaro, F.; Bearpark, M.; Heyd, J. J.; Brothers, E.; Kudin, K. N.; Staroverov, V. N.; Kobayashi, R.; Normand, J.; Raghavachari, K.; Rendell, A.; Burant, J. C.; Iyengar, S. S.; Tomasi, J.; Cossi, M.; Rega, N.; Millam, J. M.; Klene, M.; Knox, J. E.; Cross, J. B.; Bakken, V.; Adamo, C.; Jaramillo, J.; Gomperts, R.; Stratmann, R. E.; Yazyev, O.; Austin, A. J.; Cammi, R.; Pomelli, C.; Ochterski, J. W.; Martin, R. L.; Morokuma, K.; Zakrzewski, V. G.; Voth, G. A.; Salvador, P.; Dannenberg, J. J.; Dapprich, S.; Daniels, A. D.; Farkas, O.; Foresman, J. B.; Ortiz, J. V.; Cioslowski J.; Fox, D. J. Gaussian 09 Revisions A.02 and C.01, Gaussian Inc., Wallingford CT, 2009.
49. Runge, E.; Gross, E. K. U., Density-Functional Theory for Time-Dependent Systems. *Phys. Rev. Lett.* **1984,** *52*, 997-1000.
50. Casida, M. E., Time-Dependent Density Functional Response Theory for Molecules. *Recent advances in density functional methods* **1995,** *1*, 155-192.
51. Tomasi, J.; Mennucci, B.; Cammi, R., Quantum Mechanical Continuum Solvation Models. *Chem. Rev.* **2005,** *105*, 2999-3094.
52. Zhao, Y.; Truhlar, D., The M06 suite of density functionals for main group thermochemistry, thermochemical kinetics, noncovalent interactions, excited states, and transition elements: two new functionals and systematic testing of four M06-class functionals and 12 other functionals. *Theor. Chem. Acc.* **2008,** *120*, 215-241.
53. Ernzerhof, M.; Scuseria, G. E., Assessment of the Perdew–Burke–Ernzerhof exchange-correlation functional. *J. Chem. Phys.* **1999,** *110*, 5029-5036.
54. Adamo, C.; Barone, V., Toward Reliable Density Functional Methods Without Adjustable Parameters: The PBE0 Model. *J. Chem. Phys.* **1999,** *110*, 6158-6170.
55. Chai, J.-D.; Head-Gordon, M., Long-Range Corrected Hybrid Density Functionals with Damped Atom-Atom Dispersion Corrections. *Phys. Chem. Chem. Phys.* **2008,** *10*, 6615-6620.
56. Cioslowski, J., A New Population Analysis Based on Atomic Polar Tensors. *J. Am. Chem. Soc.* **1989,** *111*, 8333-8336.

57. Jacquemin, D.; Planchat, A.; Adamo, C.; Mennucci, B., TD-DFT Assessment of Functionals for Optical 0–0 Transitions in Solvated Dyes. *J. Chem. Theory Comput.* **2012,** *8*, 2359-2372.
58. Charaf-Eddin, A.; Planchat, A.; Mennucci, B.; Adamo, C.; Jacquemin, D., Choosing a Functional for Computing Absorption and Fluorescence Band Shapes with TD-DFT. *J. Chem. Theory Comput.* **2013,** *9*, 2749-2760.
59. Santoro, F.; Improta, R.; Lami, A.; Bloino, J.; Barone, V., Effective Method to Compute Franck-Condon Integrals for Optical Spectra of Large Molecules in Solution. *J. Chem. Phys.* **2007,** *126*, -.
60. Santoro, F.; Lami, A.; Improta, R.; Barone, V., Effective Method to Compute Vibrationally Resolved Optical Spectra of Large Molecules at Finite Temperature in the Gas Phase and in Solution. *J. Chem. Phys.* **2007,** *126*, -.
61. Piotto, M.; Bourdonneau, M.; Elbayed, K.; Wieruszeski, J.-M.; Lippens, G., New DEFT Sequences for the Acquisition of One-Dimensional Carbon NMR Spectra of Small Unlabelled Molecules. *Magn. Res. Chem.* **2006,** *44*, 943-947.